Multi-Poisson process analysis of real-time soft-error rate measurements in bulk 65 nm and 40 nm SRAMs

Soilihi Moindjie, Jean-Luc Autran, Daniela Munteanu, Gilles Gasiot, Philippe Roche

Multi-Poisson Process Analysis of Real-Time Soft-Error Rate Measurements in Bulk 65nm and 40nm SRAMs

S. Moindjie[a,b], J.L. Autran[a,b,*], D. Munteanu[a,b], G. Gasiot[b,c], P. Roche[b,c]

[a] *Aix Marseille Univ, Univ Toulon, CNRS, IM2NP (UMR 7334), Marseille, France*
[b] *STMicroelectronics, Crolles, France*
[c] *Radiation Effects and Electrical Reliability (REER) Joint Laboratory, AMU-CNRS-ISEN-STMicroelectronics*

Abstract

Altitude and underground real-time soft error rate (SER) measurements on SRAM circuits have been analyzed in terms of independent multi-Poisson processes describing the occurrence of single events as a function of bit flip multiplicity. Applied for both neutron-induced and alpha particle-induced SERs, this detailed analysis highlights the respective contributions of atmospheric radiation and alpha contamination to multiple cell upset mechanisms. It also offers a simple way to predict by simulation the radiation response of a given technology for any terrestrial position, as illustrated here for bulk 65nm and 40nm SRAMs.

---

[*] **Corresponding author.**
Jean-luc.autran@univ-amu.fr
Tel: +33 (0) 413 594 627

1. Introduction

Real-time soft error rate (RTSER) technique is an experimental reliability method to determine the soft error sensitivity of a given component, circuit or system [1-5]. The methodology consists in a direct observation of a large number of devices working in parallel under standard operating conditions and exposed to ambient background radiation at ground level. From the detection and counting of single events upsets occurring during the experiment, one can estimate the soft error rate (SER) of the devices under test. In case of SRAM circuits, the result can be given in terms of "event" SER, "total bit flip" SER, "multiple cell upset" (MCU) SER, and can be numerically expressed in FIT/Mbit (one FIT equals one failure per 10^9 hours of operation) [6-7].

For modern CMOS circuits at terrestrial level, SER is the result of a weighting of two main components due to: i) the atmospheric particle flux and particularly the high-energy neutrons interacting with IC materials; ii) the traces of radioactive elements present in the circuit materials, mainly U or Th contaminations at sub-ppb concentrations. These two SER components are respectively labeled neutron-SER (n-SER) and alpha-SER (α-SER). Neutron-SER is proportional to the intensity of the high-energy neutron flux at test location whereas alpha-SER is fixed and linked to the concentrations of radioactive impurities. The measured SER at a given test location is generally expressed as [6, 8]:

$$SER_{test\ location} = AF \times n\text{-}SER_{NYC} + \alpha\text{-}SER \qquad (1)$$

where AF is the so-called acceleration factor [8] which define the relative neutron flux at test location with respect to sea-level (reference New York City, NYC) and n-SER_{NYC} is the value of the neutron-SER normalized for NYC conditions. From Eq. (1), it is obvious that α-SER can be directly measured during an underground experiment (AF = 0) and that measurements at two different locations is sufficient for determining the two unknown quantities n-SER_{NYC} and α-SER.

In this study, altitude (on the ASTEP platform [9-10]), underground (at LSM, Modane [11-12]) and sea level (at IM2NP laboratory, Marseille) real-time soft error rate (SER) measurements on bulk 65nm SRAM circuits have been analyzed in terms of independent multi-Poisson processes describing the occurrence of single events as a function of bit flip multiplicity. This approach has been applied for estimating the event rates induced by atmospheric neutrons and alpha-particle emitters as a function of event multiplicity. We used these extracted results to predict by simulation the radiation response of the 65nm SRAMs for a third test location at sea-level (Marseille, France), illustrating the advantage of this method not only to evaluate the global SER value but also to accurately estimate the occurrence of MCU events as a function of their event multiplicity. Additional results concerning altitude and sea level measurements on bulk 40nm SRAMs extend the proposed analysis to the specific case of very large multiplicity events.

2. Theory

The occurrence of soft errors in electronics is a continuous time stochastic process. The principle of a RTSER experiment is to count the number of random events N(t) that have occurred up to some point t in time over a large population of circuits (the number of events is therefore small relative to the number of memory elements considered in the test). In such a real-time approach, soft errors are not permanent because they are eliminated when new data is written after detection: a RTSER test is thus equivalent to a life-test with replacement, i.e. in which a failing device is replaced with a new device immediately upon failure detection. Assuming that soft errors are also random in space (within the circuits), independent of each other and occur with a fixed event rate λ, the counting process $\{N(t), t \geq 0\}$ in a finite interval of time t consequently obeys the Poisson(λt) distribution [13]:

$$P(N(t)=n)=\frac{e^{-\lambda t}(\lambda t)^n}{n!}, \text{ n = 0, 1, 2}$$

(2)

The maximum likelihood estimate for λ is simply the number of detected events N divided by the experiment duration T and eventually normalized with respect to the number of units on test. Expressing this later quantity in Mbit for a memory test and time in MBit×h, λ can be directly estimated from:

$$\lambda = N/\Sigma \tag{3}$$

where Σ is the number of MBit×h cumulated at time T given by:

$$\Sigma=\int_0^T MEM(t)\,dt \tag{4}$$

where MEM(t) represents the number of Mbit under test at time t. This quantity may be variable in case of device automatic disconnection by the system due to abnormal current consumption or other anomaly detected at device, daugthercard or mothercard levels.

The counting process, previously introduced, can be applied to "single events" (whatever the type of these events), or more specifically to single bit upsets (SBU) or to multiple cell upsets (MCU) defined by a given event multiplicity (noted MCU(q), q = 2, 3,.. corresponding to the number of bitcells simultaneously upset during a same particle interaction event). Let $N_1(t)$, $N_2(t)$,…. $N_i(t)$, … $N_M(t)$ be M independent Poisson processes with event rates λ_1, λ_2,…, λ_i,… λ_M respectively corresponding to the counting of SBU, MCU(2), …, MCU(i),… MCU(M) events. The total event counting process $N(t) = \sum N_i(t)$ will be the merging of all these Poisson processes and will be also a Poisson process with rate $\lambda = \lambda_1 + \lambda_2 + \ldots + \lambda_i \ldots + \lambda_M$, as illustrated in Fig. 1.

Performing such a multi-Poisson process decomposition of the global "single event" process occurring during a RTSER experiment will allow us to reveal the respective contributions of atmospheric neutrons and alpha-particle emitters in the MCU SER response of the technology under test, as illustrated in the following.

3. Real-time experiments

For the purpose of this study, we considered raw data of several RTSER experiments performed on: i) 3,226 Mbit of bulk 65nm Single-Port SRAMS between 2008 and 2017; ii) 7,168 Mbit of bulk 40nm Single-Port SRAMS between 2011 and 2017. Details about these experiments can be found in Refs. [6, 10-11, 14-16]. Table I summarizes these experiments conducted on the ASTEP platform (2,255 m of altitude), at the underground laboratory of Modane (LSM) and at sea-level in Marseille (IM2NP laboratory). 65nm altitude and underground experiments were conducted in parallel with two identical setups; the setup installed in Modane was transported in Marseille in 2014 for sea level measurements. The 40nm experiments were successively performed on ASTEP and in Marseille using the same setup. Both 65nm and 40nm experiments are always running in 2017 in Marseille.

Figures 2 and 3 shows the cumulative bit flips distributions versus test duration respectively obtained for the three 65nm experiments and the two 40nm experiments. Test has been conducted under nominal operating conditions: V_{DD} = 1.2V for 65nm SRAMs (1.1V for 40nm SRAMs), room temperature, standard checkerboard test pattern. These results will serve as raw data for the multi-Poisson process analysis conducted in the next section.

4. Results and discussion

4.1. Bulk 65nm SRAMs

From raw data (bit flip distributions) shown in Figs. 2, we first extracted in Table 2 the event rate per hour and per megabit of memory (Eq. (3)) of single events as a function of the event multiplicity (an event of unit multiplicity corresponding to a single bit upset).

From Eq. (1) also valid in terms of event rate, one can consider that for a given test location:

$$\lambda_i = AF \times n\text{-}\lambda_i + \alpha\text{-}\lambda_i \qquad (5)$$

where λ_i, $n\text{-}\lambda_i$ and $\alpha\text{-}\lambda_i$ are respectively the total, neutron and alpha event rates for events of multiplicity i. i=1 corresponds to a single bit upset (SBU), i=2 to a double cell upset, etc.…).

Considering Eq. (5) for both ASTEP (AF = 6.5 averaged over the duration of the experiment) and LSM (AF = 0 when atmospheric cosmic rays are totally screened) experiments, it is then possible to extract these n-λ_i and α-λ_i values for the tested technology. This extraction is reported in Table 3 and illustrated in Fig. 4. These results show that, for this particular bulk 65nm technology, soft errors are dominated at sea level by the contribution of alpha-particle radioactivity present in IC materials up to events of multiplicity equal to 6. In particular, the alpha event rate is 6 times larger than neutron event for SBU, 7 times larger for MCU(2), 5 times larger for MCU(3) and 4 times larger for MCU(5) and MCU(6). Neutrons and alphas have finally similar event rate for MCU(4) whereas neutrons are found to dominate for larger MCUs.

In order to verify the validity of such extractions, we use on more time Eq. (5) to estimate the alpha and neutron event rates for Marseille location from data of Table 2 extracted by the combination of ASTEP and LSM results. Taking AF = 0.9 for Marseille, Table 4 shows the results of the so-called "predicted" event rates using this procedure. These values are compared to the experimental (i.e. measured) event rates and are used to "predict" the number of events vs. multiplicity for a fixed duration of 18,697 h corresponding to the measurements. Table 4 shows that these predicted values are close to the measured ones (within 10% of uncertainty for the number of detected events), demonstrating here the interest of such a multi-Poisson process analysis to calculate not only the global event rate of the circuits but also to quantify (ideally to predict) the respective contributions of MCU events as a function of event multiplicity.

4.2. Bulk 40nm SRAMs

A similar analysis has been applied to raw data related to the bulk 40nm SRAM experiments. In this case, only data related to altitude and sea-level experiments are available (Fig. 5). Table 5 summarizes the number of detected events and the estimated event rates as a function of event multiplicity. Compared to the 65nm technology, 40nm SRAMs exhibit larger multiplicity events, up to 16 and 22 cells in size, respectively detected during altitude and sea level measurements. As previously explained [15], these large multiplicity (≥5) cell upsets always involve adjacent cells preferentially distributed in columns in the physical memory array; they are the consequence of charge diffusion-collection and bipolar amplification that propagate into the silicon well directly impacted by the ionizing particle at the origin of the observed MCU.

The neutron and alpha event rates extracted from previous data are also reported in Table 5 and are shown in Fig. 5. Due to an evident lack of statistics for large MCU events that become more and more rare when their size increases, the extraction of neutron and alpha event rates has been only performed for MCU below or equal to 12 in size. Figs. 4 and 5 clearly shows the evolution of the event rates between the two technologies as a function of the event multiplicity. First, one can observe a global decrease of the alpha event rate for the 40nm with respect to the 65nm; this reduction is especially important for SBUs (reduction factor ~2) and significant up to MCU(4). Secondly, one can note a slight increase of the neutron sensitivity concerning both SBU and all MCU events (up to MCU(7)) for the 40nm technology with respect to the 65nm one. This tendency, previously reported for the global neutron and alpha SER values [11], can be here quantified for a given event multiplicity, which is important in terms of event prediction and occurrence process simulation.

5. Conclusion

In summary, we presented in this study a detailed analysis of real-time soft error rate measurements describing the occurrence of single and multiple cell upset events as independent Poisson processes running in parallel, one for each even multiplicity (i.e. event size expressed in number of cells simultaneously upset by a single particle). Combining a minimum of two distinct experiments conducted in different terrestrial environments, this approach allowed us to estimate the rates of all the events induced by both neutron-induced and alpha particle emitters as a function of their multiplicity. The proposed method has been successfully applied to quantify the respective contributions of neutrons and alpha contamination to multiple cell upset mechanisms for two SRAM technologies manufactured in CMOS bulk 65nm and 40nm, giving new lighting on the evolution of the soft error rate with integrated circuit integration.

References

[1] J.F. Ziegler and H. Puchner, "SER – History, Trends and Challenges", Cypress Semiconductor, 2004.

[2] J.L. Autran and D. Munteanu, Soft Errors: from particles to circuits, Taylor & Francis/CRC Press, 439 p., 2015.

[3] E.H. Cannon, D.D. Reinhardt, M.S. Gordon, and P.S. Makowenskyj, "SRAM SER in 90, 130 and 180 nm Bulk and SOI Technologies," IEEE International Reliability Physics Symposium, pp. 300-304, 2004.

[4] T. Heijmen, J. Verwijst, "Altitude and Underground Real-Time SER Tests of Embedded SRAM", European Conference on Radiation and Its Effects on Components and Systems (RADECS), pp. 342-347, 2009.

[5] J.L. Autran, D. Munteanu, P. Roche, G. Gasiot, S. Martinie, S. Uznanski, S. Sauze, S. Semikh, E. Yakushev, S. Rozov, P. Loaiza, G. Warot, and M. Zampaolo, "Soft-errors induced by terrestrial neutrons and natural alpha-particle emitters in advanced memory circuits at ground level", Microelectronics Reliability, vol. 50, no. 9-11, pp. 1822- 1831, 2010.

[6] J.L. Autran, D. Munteanu, G. Gasiot, P. Roche, “Introductory Invited Paper - Real-time soft-error rate measurements: A review”, Microelectronics Reliability, 2014, Vol. 54, p.1455-1476.

[7] J.L. Autran, D. Munteanu, S. Serre, and S. Sauze, "A Review of Real- Time Soft-Error Rate Measurements in Electronic Circuits", IEEE International Reliability Physics Symposium, pp. 5B.1.1-5B.1.2, 2012.

[8] JEDEC Standard "Measurement and Reporting of Alpha Particles and Terrestrial Cosmic Ray-Induced Soft Errors in Semiconductor Devices", JESD89 Arlington, VA: JEDEC Solid State Technology Association, 2006.

[9] J.L. Autran, P. Roche, J. Borel, C. Sudre, K. Castellani-Coulié, D. Munteanu, T. Parrassin, G. Gasiot, and J.P. Schoellkopf, "Altitude SEE Test European Platform (ASTEP) and First Results in CMOS 130nm SRAM", IEEE Transactions on Nuclear Science, vol. 54, no. 4, pp. 1002-1009, Aug. 2007.

[10] J.L. Autran, D. Munteanu, S. Moindjie, T. Saad Saoud, S. Sauze, G. Gasiot, P. Roche, “ASTEP (2005-2015): Ten Years of Soft Error and Atmospheric Radiation Characterization on the Plateau de Bure," Microelectronics Reliability, 2015, Vol. 55, p. 1506-1511.

[11] J.L. Autran, D. Munteanu, S. Sauze, G. Gasiot, P. Roche, “Altitude and Underground Real-Time SER Testing of SRAMs Manufactured in CMOS Bulk 130, 65 and 40 nm," 2014 IEEE Radiation Effects Data Workshop (REDW), pp.1-8, 14-18 July 2014.

[12] J.L. Autran, P. Roche, S. Sauze, G. Gasiot, D. Munteanu, P. Loaiza, M. Zampaolo, J. Borel, S. Rozov, and E. Yakushev, “Combined Altitude and Underground Real-Time SER Characterization of CMOS Technologies on the ASTEP-LSM Platform”, International Conference on Integrated Circuit Design and Technology (ICICDT 2009), pp. 113- 120, 2009.

[13] J.F.C. Kingman, Poisson Processes, Clarendon Press, 112 p., 1992.

[14] J.L. Autran, P. Roche, S. Sauze, G. Gasiot, D. Munteanu, P. Loaiza, M. Zampaolo, J. Borel, “Altitude and Underground Real-Time SER Characterization of CMOS 65nm SRAM”, IEEE Transactions on Nuclear Science, Vol. 56, 2009, Vol. 56, no. 4, p. 2258-2266.

[15] J.L. Autran, S. Serre, D. Munteanu, S. Martinie, S. Semikh, S. Sauze, S. Uznanski, G. Gasiot, L. Dugouyon, P. Roche, “Real-Time Soft-Error Testing of 40nm SRAMs”, International Reliability Physics Symposium (IRPS’2012), Anaheim, USA, April 15-19, 2012, 3C-5.

[16] J.L Autran, D Munteanu, S Moindjie, T Saad Saoud, G Gasiot, P Roche, “Real-time soft error rate measurements on bulk 40nm SRAM memories: a five-year dual-site experiment", Semiconductor Science & Technology, 2016, Vol. 31, n°11, p. 114003.

Figure and table captions

Figure 1. Merging M Poisson processes corresponding to the occurrence of single events of different cell upset multiplicities.

Figure 2. Cumulated distributions of bit flips versus time for the altitude, underground and sea level experiments on bulk 65 nm SRAMs.

Figure 3. Cumulated distributions of bit flips versus time for the altitude and sea level experiments on bulk 40 nm SRAMs.

Figure 4. Neutron and alpha event rates for the bulk 65nm SRAM technology as a function of event multiplicity as extracted in Table 5.

Figure 5. Neutron and alpha event rates for the bulk 40nm SRAM technology as a function of event multiplicity as extracted in Table 5.

Table 1. Summary of the real-time soft-error rate (RTSER) experiments considered in this study.

Table 2. Event rate extraction from RTSER data for the altitude, underground and sea level experiments on bulk 65nm SRAMs.

Table 3. Extracted values of neutron and alpha event rates as a function of event multiplicity for the 65nm SRAM technology (from data of Table 2 using Eq. (5) applied for both altitude and underground conditions).

Table 4. Comparison between extracted (Table 2) and predicted event rates (from Table 3 using Eq.(5) applied for Marseille conditions) for the sea-level experiment.

Table 5. Event rate extraction from RTSER data for the altitude and sea level experiments on bulk 40nm SRAMs. Extracted values of neutron and alpha event rates (using Eq. (5) considering altitude and sea level data) as a function of event multiplicity are also reported.

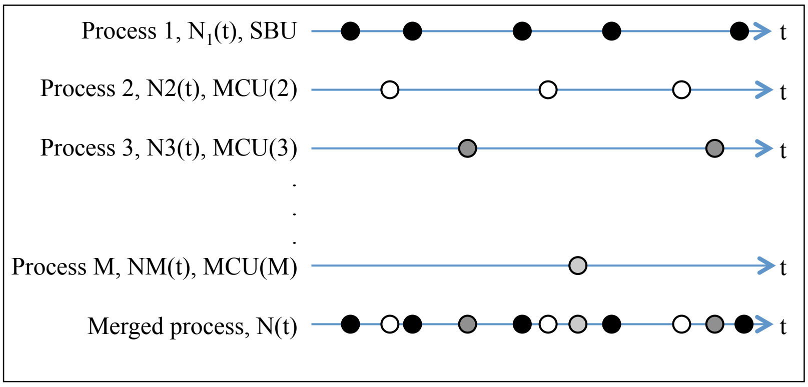

Moindjie et al. Figure 1

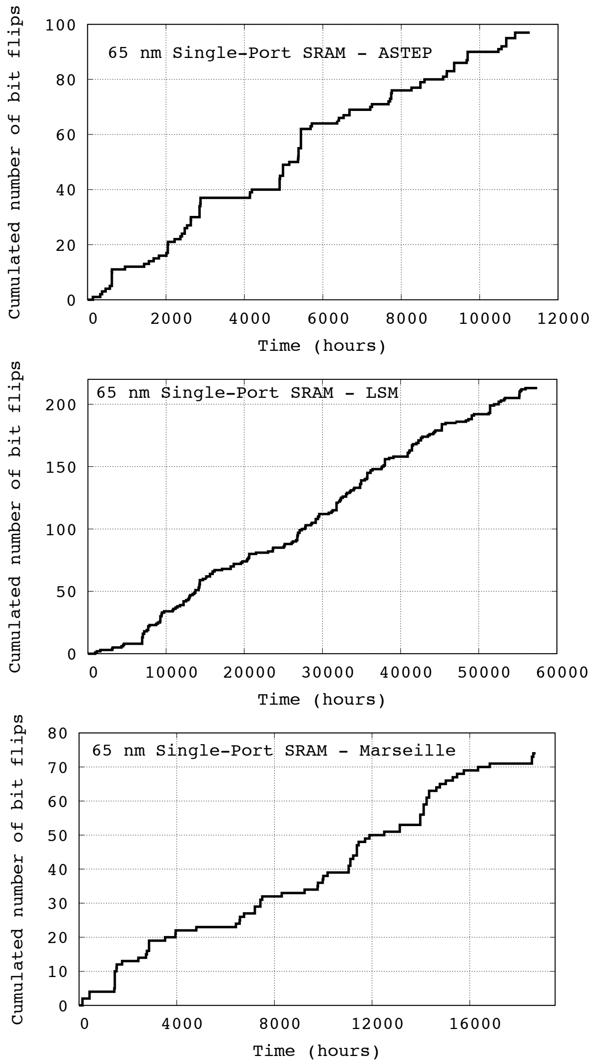

Moindjie et al. Figure 2

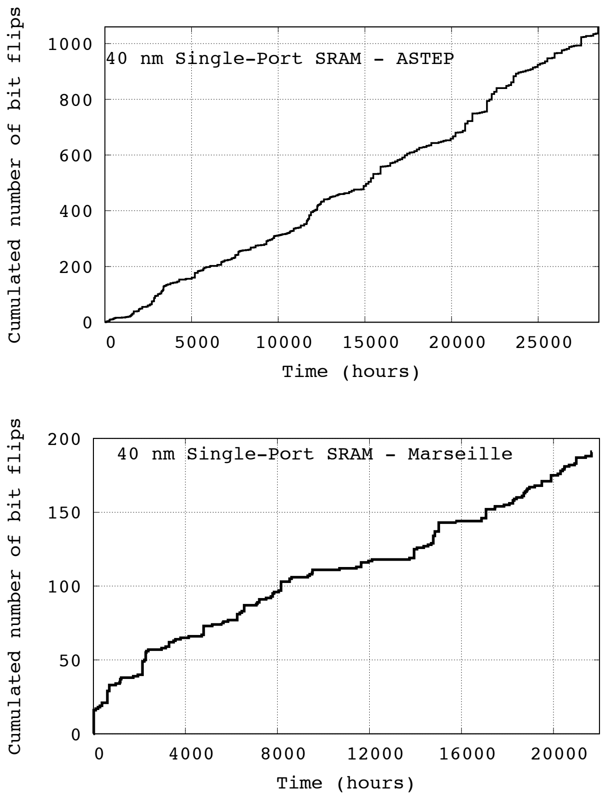

Moindjie et al. Figure 3

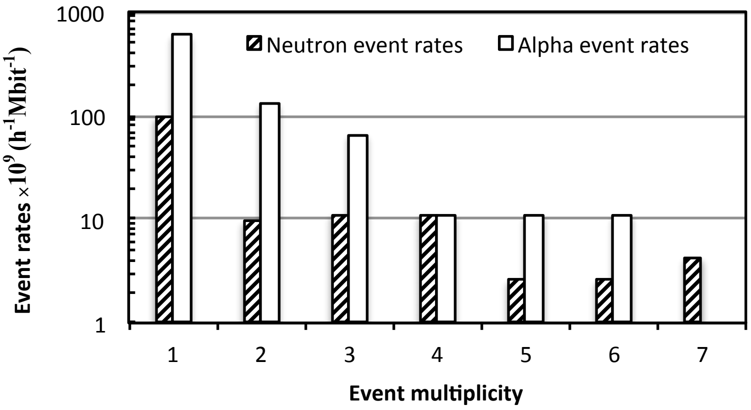

Moindjie et al. Figure 4

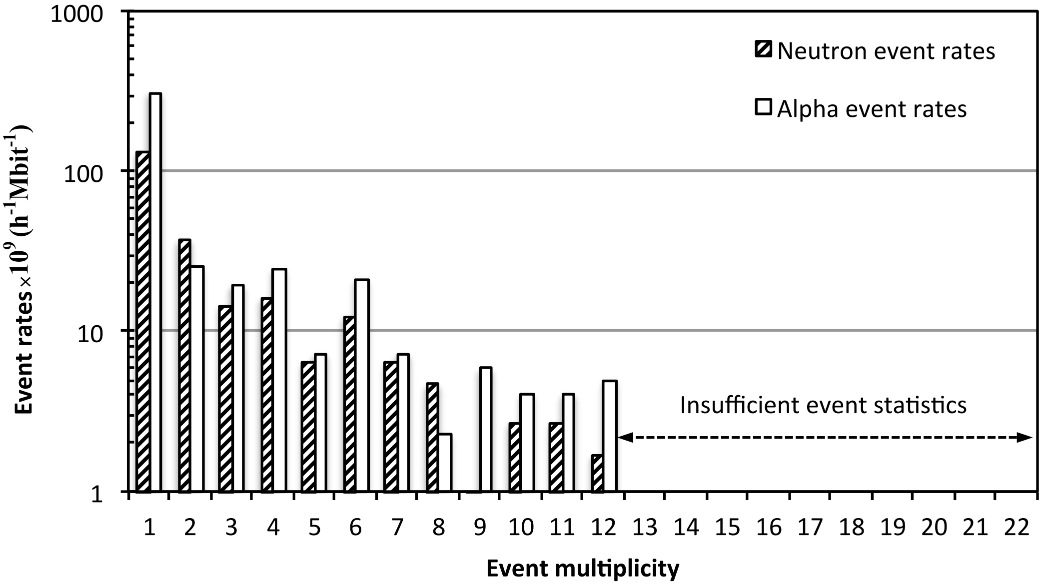

Moindjie et al. Figure 5

	Bulk 65nm SRAMs			Bulk 40nm SRAMs		
Location	Start date Stop date	Acceler. factor AF	Effective cumulated hours of tests	Start date Stop date	Acceler. factor AF	Effective cumulated hours of tests
ASTEP	01/21/2008 05/07/2009	6.5	11,278	3/11/2011 6/10/2014	6.0	28,494
LSM	04/11/2008 01/25/2015	0	57,058	–	–	–
Marseille	03/13/2015 Ongoing*	0.9	18,697	10/16/2014 Ongoing*	0.9	21,676

*Results reported on 04/30/2017

Moindjie et al. Table 1

	Bulk 65nm SRAMs					
	Altitude experiment		**Underground experiment**		**Sea level experiment**	
Event multiplicity	Number of Events	Event rate ($\times 10^{-7}$ h^{-1}Mbit^{-1})	Number of Events	Event rate ($\times 10^{-7}$ h^{-1}Mbit^{-1})	Number of Events	Event rate ($\times 10^{-7}$ h^{-1}Mbit^{-1})
1	44	$\lambda_1 = 12.1$	109	$\lambda_1 = 5.92$	36	$\lambda_1 = 5.97$
2	7	$\lambda_2 = 1.93$	24	$\lambda_2 = 1.30$	9	$\lambda_2 = 1.49$
3	5	$\lambda_3 = 1.38$	12	$\lambda_3 = 0.652$	5	$\lambda_3 = 0.829$
4	3	$\lambda_4 = 0.827$	2	$\lambda_4 = 0.109$	1	$\lambda_4 = 0.166$
5	1	$\lambda_5 = 0.276$	2	$\lambda_5 = 0.109$	1	$\lambda_5 = 0.166$
6	1	$\lambda_6 = 0.276$	2	$\lambda_6 = 0.109$	0	$\lambda_6 = 0$
7	1	$\lambda_7 = 0.276$	0	$\lambda_7 = 0$	0	$\lambda_7 = 0$

Moindjie et al. Table 2

Bulk 65nm SRAMs		
Event multiplicity	**Neutron event rate ($\times 10^{-7}$ $h^{-1}Mbit^{-1}$)**	**Alpha event rate ($\times 10^{-7}$ $h^{-1}Mbit^{-1}$)**
1	n-λ_1 = 0.955	α-λ_1 = 5.92
2	n-λ_2 = 0.096	α-λ_2 = 1.30
3	n-λ_3 = 0.112	α-λ_3 = 0.652
4	n-λ_4 = 0.112	α-λ_4 = 0.109
5	n-λ_5 = 0.026	α-λ_5 = 0.109
6	n-λ_6 = 0.026	α-λ_6 = 0.109
7	n-λ_7 = 0.004	α-λ_7 = 0

Moindjie et al. Table 3

Bulk 65nm SRAMs – Sea level measurements				
Event multi-plicity	**Number of Events**		**Event rate ($\times 10^{-7}$ h^{-1}Mbit^{-1})**	
	Measured	Predicted	Measured	Predicted
1	36	41	5.97	6.77
2	9	8	1.49	1.39
3	5	5	0.829	0.751
4	1	1	0.166	0.207
5	1	1	0.166	0.132
6	0	1	0	0.132
7	0	0	0	0.038
Total events	52	57		

Moindjie et al. Table 4

	Bulk 40nm SRAMs					
	Altitude experiment		**Sea level experiment**		**Extracted event rates**	
Event multiplicity	Number of Events	Event rate ($\times 10^{-7}$ h^{-1}Mbit^{-1})	Number of Events	Event rate ($\times 10^{-7}$ h^{-1}Mbit^{-1})	**Neutron event rate ($\times 10^{-7}$ h^{-1}Mbit^{-1})**	**Alpha event rate ($\times 10^{-7}$ h^{-1}Mbit^{-1})**
1	217	$\lambda_1 = 11.0$	66	$\lambda_1 = 4.31$	n-$\lambda_1 = 1.32$	α-$\lambda_1 = 3.12$
2	49	$\lambda_2 = 2.49$	9	$\lambda_2 = 0.587$	n-$\lambda_2 = 0.373$	α-$\lambda_2 = 0.252$
3	21	$\lambda_3 = 1.07$	5	$\lambda_3 = 0.326$	n-$\lambda_3 = 0.145$	α-$\lambda_3 = 0.196$
4	24	$\lambda_4 = 1.22$	6	$\lambda_4 = 0.391$	n-$\lambda_4 = 0.112$	α-$\lambda_4 = 0.245$
5	9	$\lambda_5 = 0.457$	2	$\lambda_5 = 0.130$	n-$\lambda_5 = 0.026$	α-$\lambda_5 = 0.072$
6	19	$\lambda_6 = 0.965$	5	$\lambda_6 = 0.326$	n-$\lambda_6 = 0.026$	α-$\lambda_6 = 0.213$
7	9	$\lambda_7 = 0.457$	2	$\lambda_7 = 0.130$	n-$\lambda_7 = 0.004$	α-$\lambda_7 = 0.072$
8	6	$\lambda_8 = 0.305$	1	$\lambda_8 = 0.065$	n-$\lambda_8 = 0.955$	α-$\lambda_8 = 0.023$
9	2	$\lambda_9 = 0.102$	1	$\lambda_9 = 0.065$	n-$\lambda_9 = 0.096$	α-$\lambda_9 = 0\ .059$
10	4	$\lambda_{10} = 0.203$	1	$\lambda_{10} = 0$	n-$\lambda_{10} = 0.112$	α-$\lambda_{10} = 0.041$
11	4	$\lambda_{11} = 0.203$	1	$\lambda_{11} = 0$	n-$\lambda_{11} = 0.112$	α-$\lambda_{11} = 0.041$
12	3	$\lambda_{12} = 0.152$	1	$\lambda_{12} = 0$	n-$\lambda_{12} = 0.026$	α-$\lambda_{12} = 0.050$
13	0	$\lambda_{13} = 0$	0	$\lambda_{13} = 0$	Insufficient event statistics for the extraction of reliable neutron and alpha event rates	
14	0	$\lambda_{14} = 0$	0	$\lambda_{14} = 0$		
15	0	$\lambda_{15} = 0$	0	$\lambda_{15} = 0$		
16	0	$\lambda_{16} = 0$	1	$\lambda_{16} = 0.065$		
17	3	$\lambda_{17} = 0.152$	0	$\lambda_{17} = 0$		
18	0	$\lambda_{18} = 0$	0	$\lambda_{18} = 0$		
19	0	$\lambda_{19} = 0$	0	$\lambda_{19} = 0$		
20	0	$\lambda_{20} = 0$	0	$\lambda_{20} = 0$		
21	1	$\lambda_{21} = 0.051$	0	$\lambda_{21} = 0$		
22	1	$\lambda_{22} = 0.051$	0	$\lambda_{22} = 0$		
TOTAL	**375**		**101**			

Moindjie et al. Table 5